Turkish Journal of Electrical Engineering & Computer Sciences

http://journals.tubitak.gov.tr/elektrik/

Research Article

Turk J Elec Eng & Comp Sci
(2016) 24: 5195 – 5209
© TÜBİTAK
doi:10.3906/elk-1409-88

Video temporal error concealment using improved directional boundary matching algorithm

Seyed Mojtaba MARVASTI-ZADEH, Hossein GHANEI-YAKHDAN*
Department of Electrical and Computer Engineering, Yazd University, Yazd, Iran

Received: 13.09.2014 • **Accepted/Published Online:** 07.11.2015 • **Final Version:** 06.12.2016

Abstract: Nowadays some systems such as multimedia systems try to present a high quality of digital videos every day. Because of the possible errors in communication channels, compressed video data would be damaged in the sending process. Error concealment is a useful technique for concealing the effects of sending errors at the decoder. In this paper, an improved directional boundary matching algorithm is presented, in which by using adjacent macroblocks (MBs) of the damaged MB a direction is identified for each boundary. Then every boundary of candidate MBs is compared to an identified direction. Finally, the candidate motion vector (MV) that has the minimum improved directional matching function is selected as the MV of the damaged MB. Furthermore, to increase the accuracy in damaged MV estimation, a specific weight is given to the boundaries of adjacent MBs. Conforming to the experimental results, the proposed algorithm not only outperforms subjective visual evaluation compared to classic boundary matching, outer boundary matching, and directional boundary matching algorithms, but also it is able to improve the objective quality of reconstructed video frames effectively.

Key words: Temporal error concealment, motion vector estimation, boundary matching, macroblock

1. Introduction

Transmitting compressed video data over error-prone channels causes error and reduces the visual quality of received video. Because error control methods (which are used at the encoder) will reduce the efficiency of video coding faced with limited bandwidth of communication channels, the use of these methods is not suitable.

To achieve better quality for the received videos and reduce the error effects, error concealment techniques have been presented at the decoder. Error concealment methods do not cause the increasing of the requested bandwidth and delay in retransmitting of the video bit-stream. Therefore, these methods are suitable for real-time video communications. Error concealment methods are divided into three main categories: spatial domain [1,2], temporal domain [3–5], and frequency domain [6,7].

Spatial and temporal error concealment techniques use spatial redundancies among pixels of the image and temporal redundancies among the consecutive frames to recover the damaged macroblocks (MBs), respectively. Frequency error concealment techniques use frequency domain data of adjacent MBs (e.g., DCT coefficients) to retrieve the damaged MBs.

Combining these methods makes hybrid [8,9], and adaptive [10] methods. Combined with different temporal, spatial, and frequency methods, these methods attempt to improve the presented results using a single method.

*Correspondence: hghaneiy@yazd.ac.ir

The easiest method of temporal error concealment is temporal replacement (TR) [11], which replaces all damaged MVs with zeros. This method is just useful for video sequences with low motion and is applied in video conferences, supervision or care protection, etc. In [12], an error concealment algorithm of whole frame loss was proposed for further refining of the TR method.

In [13], the performance of the five conventional temporal error concealment techniques for reconstructing the damaged frames in critical situations was analyzed. These techniques were analyzed according to two similarity metrics (namely sum of absolute differences for boundary matching (SAD-BM) and sum of absolute differences for out boundary matching (SAD-OBM)) and the best approaches to use in mobile video applications were selected.

One of the most common temporal error concealment algorithms is the classic boundary matching algorithm (BMA) [14]. This algorithm supposes that luminance differences in boundaries of damaged MBs can change smoothly. However, this algorithm has noticeable limitations. When all the adjacent boundaries do not exist, performance will be decreased. In addition, whenever adjacent pixels have sudden changes, the BMA performance will be decreased.

According to the BMA criterion with reliability coefficient, two of the best MVs were selected in the double-weighted MV algorithm [15]. Then the optimal MV was calculated by weighting the MVs in terms of their accuracy. In [16], a method was presented for MV optimization of a damaged MB with the two best MVs obtained from the BMA. Furthermore, in this method, a preprocessing algorithm was presented for determining a better MV set. A Kalman filter-based error concealment method [17] estimates the MVs of damaged MBs (which are obtained by the BMA) with more accuracy. In this method, MVs in successive MBs and the Kalman filter are considered with an appropriate state-space variable and a corrector of measurement errors.

To evaluate the candidate MBs for error concealment, an efficient boundary matching algorithm [18] utilizes classic and proposed boundary matching criteria to use the spatial and temporal redundancy among video frames, adaptively. According to the error concealment priority list (which is determined by the algorithm), the algorithm performs error concealment of each video frame more accurately.

The outer boundary matching algorithm (OBMA) [19] uses the spatial and temporal smoothness of damaged MB boundaries along with a linear translational model to conceal the damaged MB. Unlike the BMA, the sudden changes in boundary pixels help the OBMA to select a correct MB. In addition, the dynamic temporal error concealment [20] uses different methods based on the motion in specific areas of video frames that is regular, irregular, or zero. Furthermore, the method selects an adaptive candidate MV set and utilizes the TR, adjacent MV, or improved OBMA methods to estimate the damaged MV.

An adaptive error concealment mechanism [21] uses different error concealment methods based on spatial and temporal information of the video sequences. According to the instantaneous sequence characteristics and the error pattern, a decision tree selects a suitable error concealment method for estimating the damaged MBs. This mechanism is useful for mobile video streaming applications. Furthermore, an efficient adaptive boundary matching algorithm [22] simultaneously uses two boundary matching criteria (namely the outer boundary matching criterion (OBMC) and directional temporal boundary matching criterion (DTBMC)) to estimate more accurately the damaged MBs.

An efficient spatiotemporal boundary matching algorithm (ESTBMA) [23] exploits a more general match distortion function. This function calculates spatial boundary-match distortion (BMA distortion function), temporal boundary-match distortion (OBMA distortion function), and side-match distortion with the weighting factors. Finally, the best MV for the damaged MB is estimated by minimizing the general distortion function.

A dynamic multimode switching (DMS) algorithm [24] uses different error concealment modes based on different features of intra- and interframes adaptively. In order to perform temporal error concealment, the algorithm utilizes the adaptive boundary matching criterion, which includes a directional boundary matching algorithm (DBMA) and external boundary matching algorithm (EBMA). If the number of edge points in the adjacent boundary of the candidate MB is greater than the threshold (which is experimentally selected), the criterion selects the DBMA.

The DBMA determines the comparison direction for each boundary pixel of the candidate MB. In order to improve the accuracy of damaged MV estimation, every boundary pixel in the determined direction is compared to the pixel of the outer boundary of the damaged MB. However, the performance of this method decreases extremely if the candidate MVs are not accurate (e.g., they are obtained from the results of the last error concealment's stages or inappropriate candidate MVs sets). Moreover, this algorithm assumes that the direction of edges in boundaries of damaged MBs did not change in comparison to the reference frame. Therefore, if these conditions are not satisfied, this algorithm does not have satisfactory results.

In this paper, an improved directional boundary matching algorithm is proposed for resolving DBMA problems and accuracy increasing in the estimation of the damaged MVs. With the smoothness assumption in boundaries of damaged MBs, the proposed algorithm uses outer boundaries of the damaged MB in the current frame to determine a comparison direction of boundary pixels. Furthermore, the proposed algorithm leads to a decrease in computational complexity and makes it faster than DBMA by determining just one dominant direction for comparison of each boundary from the damaged MB (not for each boundary pixel from each candidate MB). Moreover, according to the reliability of each outer boundary from the damaged MB, there is a specific weight for each boundary. These weights assign different importance to the determined directions from adjacent boundaries and cause the low error in the boundary matching process. Therefore, considering the specific weight for each boundary in the boundary matching criterion can lead to more accuracy and low error propagation.

This paper is organized as follows. First, the DBMA is described in Section 2. Section 3 explains the proposed algorithm. After that, the experimental results are presented in Section 4, and, finally, the conclusion is summarized in Section 5.

2. Directional boundary matching algorithm (DBMA)

This algorithm (like the BMA) uses a spatial smoothness feature on boundaries of the damaged MB to find the best candidate MV. In this algorithm, a correct direction is identified for each boundary pixel of the candidate MB. This direction is identified using two inner boundaries of the candidate MB. Then each boundary pixel of the candidate MB is compared with the identified direction of outer boundary pixels of the damaged MB. Thus, the estimation of the damaged MV is more accurate. Figure 1a shows the comparison of boundaries in the BMA. In addition, Figure 1b represents the way of edge direction identification for each top boundary pixel in the reference frame and the method for comparing them with boundary pixels of the current frame in DBMA.

The boundary matching process for estimating of the damaged MB using the DBMA is as follows. First, the correct direction for comparing each kth pixel in (i,j) coordinates in each boundary (E_{dir}^{k}) is calculated by:

$$E_{dir}^{k} = min\left(E_{k-1}\left(dir\right), E_{k}\left(dir\right), E_{k+1}\left(dir\right)\right)\ ;\ dir \in \{t,\, l,\, b,\, r\}\,. \tag{1}$$

The kth pixel can be in each top, left, bottom, or right boundary, which is indicated with t, l, b, or r, respectively. Also, $E_{k-1}(.)$, $E_{k}(.)$, $E_{k+1}(.)$ are absolute difference values among the kth pixel and the k-

*1*th, *k*th, and *k+1*th pixels in the second boundary of the candidate MB, respectively. These differences are calculated in the top, left, bottom, and right boundary by Eqs. (2) through (5), respectively.

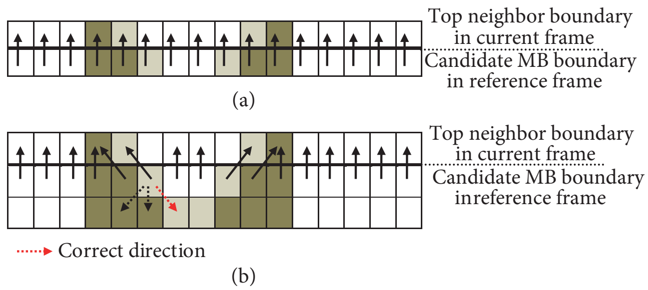

Figure 1. Illustration of top boundary matching.

$$\left\{\begin{array}{l} E_{k-1}\left(t\right)=\left|f_{ref}\left(i+vi,j+vj\right)-f_{ref}\left(i+vi-1,j+vj+1\right)\right| \\ E_{k}\left(t\right)=\left|f_{ref}\left(i+vi,j+vj\right)-f_{ref}\left(i+vi,j+vj+1\right)\right| \\ E_{k+1}\left(t\right)=\left|f_{ref}\left(i+vi,j+vj\right)-f_{ref}\left(i+vi+1,j+vj+1\right)\right| \end{array}\right. \tag{2}$$

$$\left\{\begin{array}{l} E_{k-1}\left(l\right)=\left|f_{ref}\left(i+vi,j+vj\right)-f_{ref}\left(i+vi+1,j+vj-1\right)\right| \\ E_{k}\left(l\right)=\left|f_{ref}\left(i+vi,j+vj\right)-f_{ref}\left(i+vi+1,j+vj\right)\right| \\ E_{k+1}\left(l\right)=\left|f_{ref}\left(i+vi,j+vj\right)-f_{ref}\left(i+vi+1,j+vj+1\right)\right| \end{array}\right. \tag{3}$$

$$\left\{\begin{array}{l} E_{k-1}\left(b\right)=\left|f_{ref}\left(i+vi,j+vj+S-1\right)-f_{ref}\left(i+vi-1,j+vj+S-2\right)\right| \\ E_{k}\left(b\right)=\left|f_{ref}\left(i+vi,j+vj+S-1\right)-f_{ref}\left(i+vi,j+vj+S-2\right)\right| \\ E_{k+1}\left(b\right)=\left|f_{ref}\left(i+vi,j+vj+S-1\right)-f_{ref}\left(i+vi+1,j+vj+S-2\right)\right| \end{array}\right. \tag{4}$$

$$\left\{\begin{array}{l} E_{k-1}\left(r\right)=\left|f_{ref}\left(i+vi+S-1,j+vj\right)-f_{ref}\left(i+vi+S-2,j+vj-1\right)\right| \\ E_{k}\left(r\right)=\left|f_{ref}\left(i+vi+S-1,j+vj\right)-f_{ref}\left(i+vi+S-2,j+vj\right)\right| \\ E_{k+1}\left(r\right)=\left|f_{ref}\left(i+vi+S-1,j+vj\right)-f_{ref}\left(i+vi+S-2,j+vj+1\right)\right| \end{array}\right. \tag{5}$$

Here, $f_{ref}(.,.)$ is the indicator of the reference frame and $MV(vi,vj)$ is the candidate MV. In addition, S is the number of available pixels in each boundary. Then the boundary pixel of the candidate MB in the identified direction is compared with the outer boundary pixel of the damaged MB by the following.

$$D_k^t=\left\{\begin{array}{ll} \left|f_{ref}\left(i+vi,j+vj\right)-f_{cur}\left(i+1,j-1\right)\right| & \text{if} \quad E_{dir}^k=E_{k-1} \\ \left|f_{ref}\left(i+vi,j+vj\right)-f_{cur}\left(i,j-1\right)\right| & \text{if} \quad E_{dir}^k=E_{k} \\ \left|f_{ref}\left(i+vi,j+vj\right)-f_{cur}\left(i-1,j-1\right)\right| & \text{if} \quad E_{dir}^k=E_{k+1} \end{array}\right. \tag{6}$$

$$D_k^l=\left\{\begin{array}{ll} \left|f_{ref}\left(i+vi,j+vj\right)-f_{cur}\left(i-1,j+1\right)\right| & \text{if} \quad E_{dir}^k=E_{k-1} \\ \left|f_{ref}\left(i+vi,j+vj\right)-f_{cur}\left(i-1,j\right)\right| & \text{if} \quad E_{dir}^k=E_{k} \\ \left|f_{ref}\left(i+vi,j+vj\right)-f_{cur}\left(i-1,j-1\right)\right| & \text{if} \quad E_{dir}^k=E_{k+1} \end{array}\right. \tag{7}$$

$$D_k^b = \begin{cases} |f_{ref}(i+vi, j+vj+S-1) - f_{cur}(i+1, j+S)| & \text{if} \quad E_{dir}^k = E_{k-1} \\ |f_{ref}(i+vi, j+vj+S-1) - f_{cur}(i, j+S)| & \text{if} \quad E_{dir}^k = E_k \\ |f_{ref}(i+vi, j+vj+S-1) - f_{cur}(i-1, j+S)| & \text{if} \quad E_{dir}^k = E_{k+1} \end{cases} \tag{8}$$

$$D_k^r = \begin{cases} |f_{ref}(i+vi+S-1, j+vj) - f_{cur}(i+S, j+1)| & \text{if} \quad E_{dir}^k = E_{k-1} \\ |f_{ref}(i+vi+S-1, j+vj) - f_{cur}(i+S, j)| & \text{if} \quad E_{dir}^k = E_k \\ |f_{ref}(i+vi+S-1, j+vj) - f_{cur}(i+S, j-1)| & \text{if} \quad E_{dir}^k = E_{k+1} \end{cases} \tag{9}$$

$$D_F^p = \sum_{n=0}^{S-1} D_n^p \; ; \quad p \in \{t,\, l,\, b,\, r\} \tag{10}$$

Here, $f_{cur}(.,.)$ is the indicator of the current frame and D_k^t, D_k^l, D_k^b, and D_k^r are absolute differences for each pixel in the determined direction in the top, left, bottom, and right boundary, respectively. In Eq. (10), D_F^p is used for calculating the direction distortion for each boundary. Finally, the value of the directional matching function (DMF_{DBMA}) for each candidate MB is:

$$DMF_{DBMA} = D_F^t + D_F^b + D_F^l + D_F^r, \tag{11}$$

where D_F^t, D_F^l, D_F^b, and D_F^r are the values of direction distortion for the top, left, bottom, and right boundary, respectively. At the end, the candidate MV that causes the minimum value of the DMF_{DBMA} is selected as the MV of the damaged MB.

3. Proposed algorithm

To concentrate on the temporal error concealment algorithm's design, we considered that the damaged MBs' positions in video sequences are known. Several techniques for error detection in image and video frames and for determining the position of the damaged MBs were studied in [25]. These techniques can be employed to detect the locations of damaged MBs effectively. The block diagram of the proposed algorithm is shown in Figure 2. According to this figure, a set of candidate MVs is selected after getting the coordinate of the damaged MB. This set includes adjacent MVs of the damaged MB, their mean and median MVs, the zero MV, and the corresponding MV of the damaged MB from the last frame.

Instead of selecting the direction for each pixel, the proposed algorithm uses only the dominant direction in each boundary. In addition, this algorithm identified the comparison direction of each boundary according to comparison of the two outer boundaries of the damaged MB. In this algorithm, all the boundaries of candidate MBs are compared to the last specific direction. The boundary matching process of the proposed algorithm is as follows. In the proposed algorithm, the comparison direction of each boundary is determined by:

$$E(p) = min\left(E_{ver}^p, E_{diag}^p, E_{antidiag}^p\right) \; ; \quad p \in \{t,\, l,\, b,\, r\}\,, \tag{12}$$

where E_{ver}^p, E_{diag}^p, and $E_{antidiag}^p$ are the normalized values obtained from the vertical, diagonal, and antidiagonal comparison of each boundary, respectively. As an example, these values for the top boundary are determined by Eq. (13).

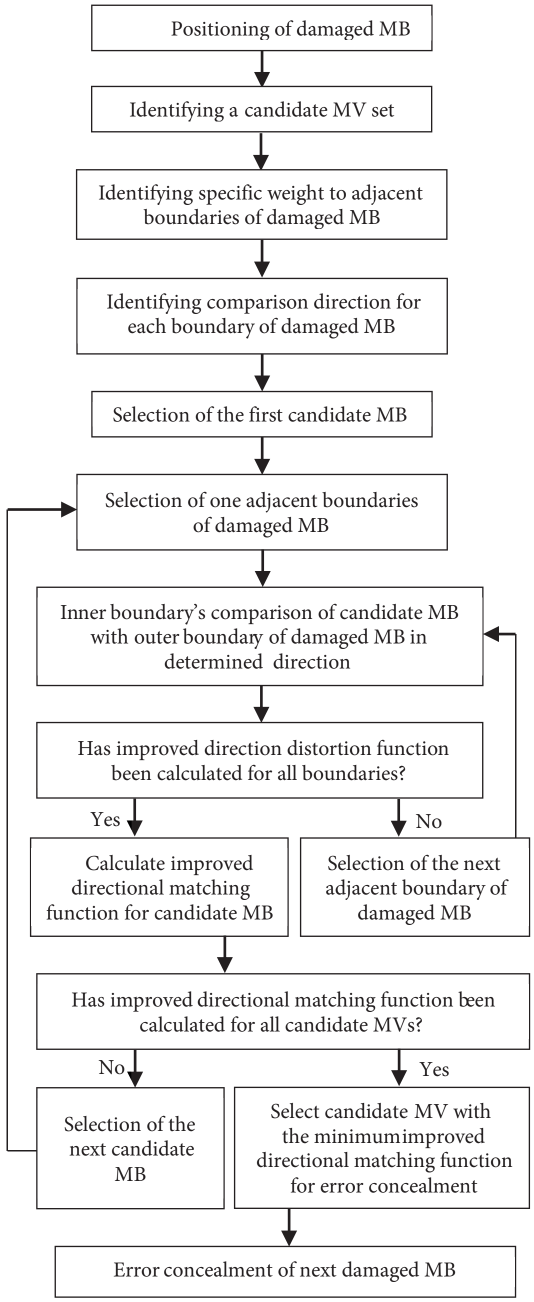

Figure 2. Block diagram of the proposed algorithm.

$$\begin{cases} E^t_{ver} = \left(\sum_{n=0}^{S-1} \left|f_{cur}\left(i+n,j-1\right) - f_{cur}\left(i+n,j-2\right)\right|\right) \Big/ S \\ E^t_{diag} = \left(\sum_{n=0}^{S-2} \left|f_{cur}\left(i+n+1,j-1\right) - f_{cur}\left(i+n,j-2\right)\right|\right) \Big/ (S-1) \\ E^t_{antidiag} = \left(\sum_{n=1}^{S-1} \left|f_{cur}\left(i+n-1,j-1\right) - f_{cur}\left(i+n,j-2\right)\right|\right) \Big/ (S-1) \end{cases} \tag{13}$$

The boundary matching process to find the best comparison direction and calculate the boundary distortion in the top boundary is shown in Figure 3. According to Figures 3a-1, 3a-2, and 3a-3, the proposed algorithm chooses one of the vertical, diagonal, or antidiagonal directions, respectively. Then the proposed algorithm performs boundary matching process in the dominant direction for every candidate MB according to Figures 3b-1, 3b-2, and 3b-3. The proposed algorithm also determines the comparison direction just once for each boundary of the damaged MB. The boundary matching process for the top boundary is as follows.

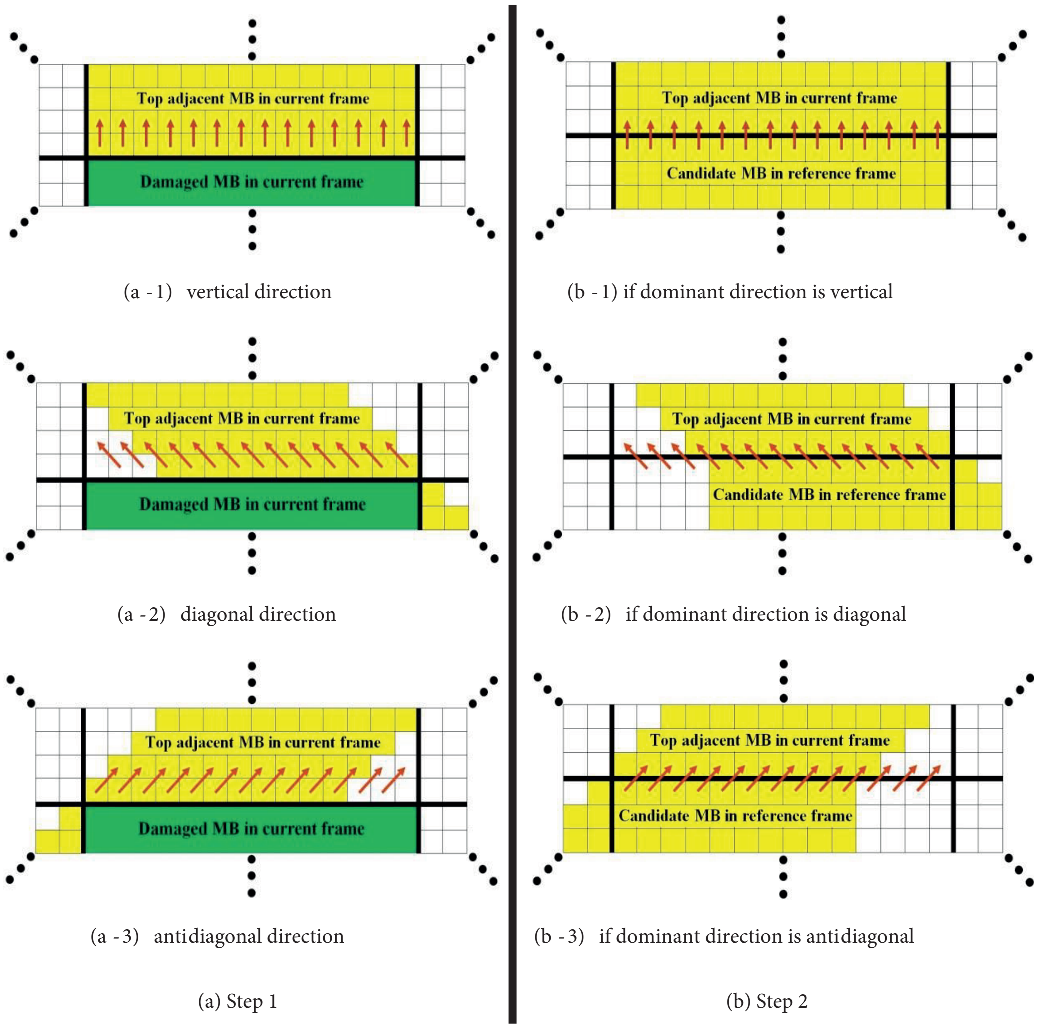

Figure 3. Illustration of top boundary matching in the proposed algorithm.

$$D_t = \begin{cases} \left(w_t \times \sum_{n=0}^{S-1} \left|f_{ref}\left(i+vi+n, j+vj\right) - f_{cur}\left(i+n, j-1\right)\right|\right) \Big/ S & \text{if} \quad E(t) = E_{ver}^t \\ \left(w_t \times \sum_{n=0}^{S-2} \left|f_{ref}\left(i+vi+n+1, j+vj\right) - f_{cur}\left(i+n, j-1\right)\right|\right) \Big/ (S-1) & \text{if} \quad E(t) = E_{diag}^t \\ \left(w_t \times \sum_{n=1}^{S-1} \left|f_{ref}\left(i+vi+n-1, j+vj\right) - f_{cur}\left(i+n, j-1\right)\right|\right) \Big/ (S-1) & \text{if} \quad E(t) = E_{antidiag}^t \end{cases} \tag{14}$$

In Eq. (14), D_t is the value of the improved direction distortion function for the top boundary of the damaged MB. Furthermore, w is the weight of each outer boundary from the damaged MB. This weight is considered “1” when the adjacent MB in the current frame is available, and “0” otherwise. In addition, the weight is "0.5" for the adjacent MB, which has been obtained from previous error concealment stages. Similarly, determination of the dominant direction and calculation of the improved direction distortion function are performed for other boundaries.

The final value of the improved directional matching function ($IDMF_{Proposed}$) is calculated for each candidate MB by Eq. (15).

$$IDMF_{Proposed} = sum\ (D_p)\ ;\ \ p \in \{t, l, b, r\} \tag{15}$$

Finally, the candidate MV with the minimum value of the $IDMF_{Proposed}$ is selected as the MV of the damaged MB.

4. Experimental results

The capability of the proposed algorithm was compared with the BMA, OBMA, and DBMA, which were simulated (according to [14], [19], and [24], respectively) by the authors. The performance of the algorithms were evaluated on various types of CIF (352 × 288) video test sequences including "Mother-daughter", "Foreman", "Bus", "Ice", "Soccer", and "Hall" and also QCIF (176 × 144) video test sequences including "Mother-daughter", "Foreman", "Suzie", "Walk", "Car-phone", and "Stefan".

The video test sequences were encoded in 4:2:0 format. The size of an MB is 16 × 16. To calculate MVs, the block matching algorithm [26] with exhaustive search (full search) and the search parameter equal to seven (p = 7) were used. The errors in video frames were created with MB missing rates of 5%, 10%, and 20% in each frame randomly. For increasing the validity of the results, the experiments for every algorithm were done 20 times and the average values were used as the final results.

The average peak signal-to-noise ratio (PSNR) values (in dB) of the luminance component for 60 frames of CIF sequences and 120 frames of QCIF sequences are listed in Tables 1 and 2, respectively. To quantify the computational complexity, the execution time for each error concealment algorithm was measured with the same PC (Intel Core i5, 2.4 GHz). The average reconstruction times (in ms) for 60 frames of CIF sequences and 120 frames of QCIF sequences with average MB missing rate of 10% for different algorithms are presented in Table 3.

According to Table 1, the proposed algorithm yields higher average PSNR performance than the BMA, DBMA, and OBMA in both CIF and QCIF resolutions. From Table 1, it is observed that the proposed algorithm in CIF resolution is able to provide up to 1.3750, 1.2601, and 1.0687 dB higher PSNR than the BMA, DBMA, and OBMA, respectively. In addition, the proposed algorithm in QCIF resolution is able to provide up to 0.9994, 0.9686, and 0.8675 dB higher PSNR than the BMA, DBMA, and OBMA, respectively. From Tables 1–3, we can observe that the proposed algorithm estimates the MVs of the damaged MBs without any considerable increase in computational complexity compared to the BMA, DBMA, and OBMA.

Figures 4a–4f show the PSNR values for reconstructed CIF test sequences of "Foreman", "Mother-daughter", "Bus", "Ice", "Soccer", and "Hall", respectively. In addition, Figures 5a–5f show the PSNR values for the reconstructed QCIF test sequences of "Mother-daughter", "Foreman", "Suzie", "Walk", "Car-phone", and "Stefan", respectively. A comparison of PSNR performances versus the number of frames in Figure 4 indicates that the proposed algorithm increases the PSNR for CIF test sequences in some frames by about 4.8894, 4.5296, and 4.4812 dB compared to the BMA, DBMA, and OBMA methods, respectively. On the other hand, according to Figure 5 the proposed algorithm increases the PSNR for QCIF test sequences in some frames by about 7.4689, 7.3336, and 6.0904 dB compared to the BMA, DBMA, and OBMA methods, respectively.

Table 1. Average PSNR values for CIF video test sequences with different error concealment algorithms.

Video sequence	Error concealment algorithm	Average MB missing rate		
		5%	10%	20%
Foreman	BMA	41.5796	38.7866	35.8689
	DBMA	41.6956	39.0044	36.0818
	OBMA	42.2463	39.1593	36.2087
	Proposed algorithm	42.3105	39.5122	36.5889
Mother-daughter	BMA	43.3963	40.6027	37.9359
	DBMA	43.4679	40.7770	38.0758
	OBMA	43.9756	41.0738	38.4234
	Proposed algorithm	44.4147	41.7302	39.1687
Bus	BMA	38.2051	35.2703	32.1448
	DBMA	38.2276	35.3852	32.1754
	OBMA	38.7390	35.5766	32.3217
	Proposed algorithm	39.3114	36.6453	33.2581
Ice	BMA	42.7338	40.1444	35.9645
	DBMA	42.8049	40.1889	35.9684
	OBMA	42.9768	40.2541	35.9930
	Proposed algorithm	43.5815	41.0207	36.9974
Soccer	BMA	36.8892	33.8915	30.6722
	DBMA	37.2772	34.0893	30.8391
	OBMA	37.7666	34.3850	31.0119
	Proposed algorithm	38.0732	35.2625	31.9378
Hall	BMA	39.0875	35.6938	33.7126
	DBMA	39.1164	35.7464	33.7947
	OBMA	39.2574	35.8418	33.6478
	Proposed algorithm	39.3191	36.0090	34.1443

Table 2. Average PSNR values for QCIF video test sequences with different error concealment algorithms.

Video sequence	Error concealment algorithm	Average MB missing rate		
		5%	10%	20%
Mother-daughter	BMA	59.1776	54.9364	50.5677
	DBMA	60.9471	54.9768	50.5845
	OBMA	61.1215	55.0674	50.6323
	Proposed algorithm	61.6112	55.3514	51.0993
Foreman	BMA	57.4995	50.1073	45.4618
	DBMA	57.6424	50.1639	45.5431
	OBMA	57.6763	50.2716	45.6135
	Proposed algorithm	57.7773	50.5175	46.1842
Suzie	BMA	58.4640	53.3222	49.3099
	DBMA	58.4748	53.4058	49.3594
	OBMA	58.7133	53.6794	49.5443
	Proposed algorithm	58.8115	53.8248	49.8409
Walk	BMA	49.5189	44.0389	39.3806
	DBMA	49.5596	44.1154	39.4114
	OBMA	49.8152	44.1610	39.5125
	Proposed algorithm	50.1473	44.9537	40.3800
Car-phone	BMA	55.0912	49.9890	45.0591
	DBMA	55.1468	50.0386	45.2297
	OBMA	55.2842	50.1360	45.2510
	Proposed algorithm	55.3800	50.6149	45.8182
Stefan	BMA	50.4842	44.5438	38.1649
	DBMA	50.5262	44.6811	38.2485
	OBMA	50.6303	44.8238	38.4266
	Proposed algorithm	50.7676	45.0274	38.5335

Table 3. Average reconstruction time per MB (ms) for average MB missing rate of 10%.

Video resolution	Video sequence	Error concealment algorithm			
		BMA	DBMA	OBMA	Proposed algorithm
CIF	Foreman	2.6083	3.2847	2.5969	3.0237
	Mother-daughter	2.7011	3.3648	2.6997	3.1757
	Bus	2.6629	3.3272	2.6466	3.0575
	Ice	2.6385	3.2698	2.5784	3.1565
	Soccer	2.6452	3.2856	2.5899	3.1680
	Hall	2.7099	3.3204	2.6075	3.2346
QCIF	Mother-daughter	1.7505	2.0340	1.7452	1.9455
	Foreman	1.8923	2.2329	1.8976	2.1136
	Suzie	1.8096	2.0742	1.8032	2.0026
	Walk	1.7233	2.2754	1.7707	2.2113
	Car-phone	1.7208	2.2069	1.7327	2.1441
	Stefan	1.7526	2.2009	1.7030	2.1541

Common error concealment algorithms based on boundary matching have significant limitations. In most of these methods (such as BMA), a direction is not determined for comparison of boundary pixels in the boundary matching process. Therefore, these algorithms have acceptable performance only if the damaged MB is on vertical and horizontal edges. Otherwise, the amount of errors in the boundary matching process increases and, as a result, it decreases the accuracy of the estimated MV.

Moreover, the DBMA has some serious problems. In the DBMA, the direction of comparison for each pixel is identified by two inner boundaries of the candidate MB. There may be some of these MBs from error concealment of the reference frame. Therefore, selection of comparison direction from boundary pixels of the candidate MBs can cause low accuracy in the boundary matching process. The DBMA assumes that the obtained directions of the reference frame are protected in the current frame. However, in real conditions, many of these directions may change in the current frame. This problem may cause the reduction in estimation accuracy of damaged MVs and quality of the reconstructed video. If the assumptions in the DBMA are not satisfied, its performance may be even lower than that of the BMA.

In addition, the criterion function of the OBMA in the boundary matching process gives equal importance to the boundaries of adjacent MBs. Because some of the adjacent MBs may be from the previous stages of error concealment, these boundaries cause low accuracy in the matching process. Therefore, the proficiency of the OBMA in the estimation of damaged MVs decreases. As a result, it can cause error propagation in estimating the consecutive damaged MVs. Moreover, when the consecutive video frames have low temporal correlation, the algorithm's performance dramatically declines.

In the proposed algorithm, the boundary comparison's direction of the damaged MB is determined according to outer boundaries of the damaged MB. These boundaries are compared in three directions: vertical, diagonal, and antidiagonal. Then one of these directions is determined as a dominant direction (for comparison of each boundary from the damaged MB) and it is used in the boundary matching process. As already mentioned, the DBMA determines the direction of boundary comparison for each pixel from each boundary of the candidate MB. According to the assumption of the DBMA and the proposed algorithm that is based on high spatial correlation of image pixels, direction determination is not necessary for each boundary pixel. Therefore, the proposed algorithm with suitable approximation determines a direction of boundary comparison just once for each boundary of the damaged MB. This leads to low computational complexity and makes the proposed algorithm faster than the DBMA.

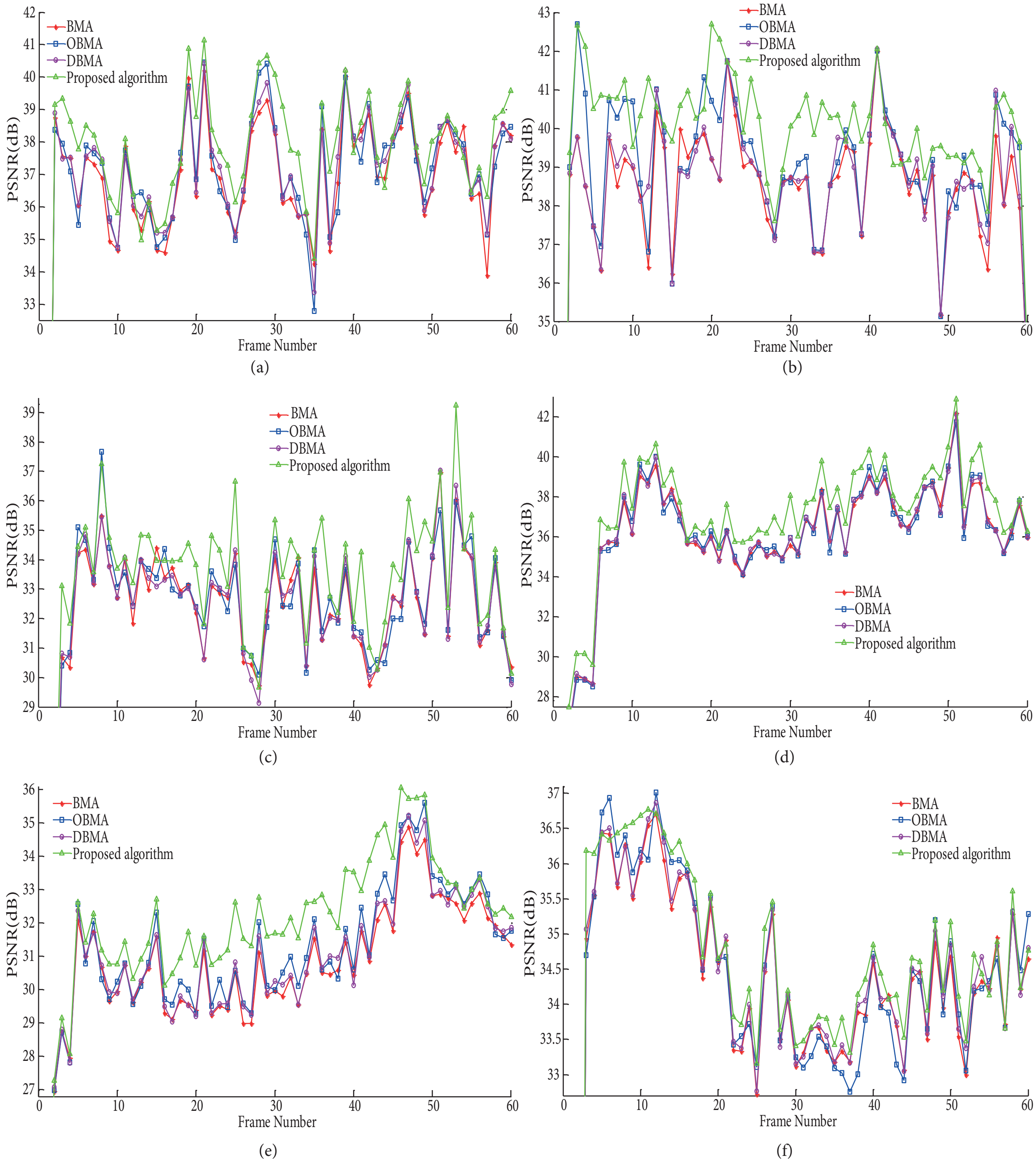

Figure 4. PSNR values of different CIF video test sequences with average MB missing rate of 20%.

According to outer boundaries of the damaged MB, the proposed algorithm selects the comparison directions and causes more accuracy in the comparison process. Therefore, change in the directions of boundary pixels' comparison compared to the reference frame does not have any effect on the boundary matching process. In addition, the proposed algorithm with considering a specific weight for each adjacent boundary of the damaged

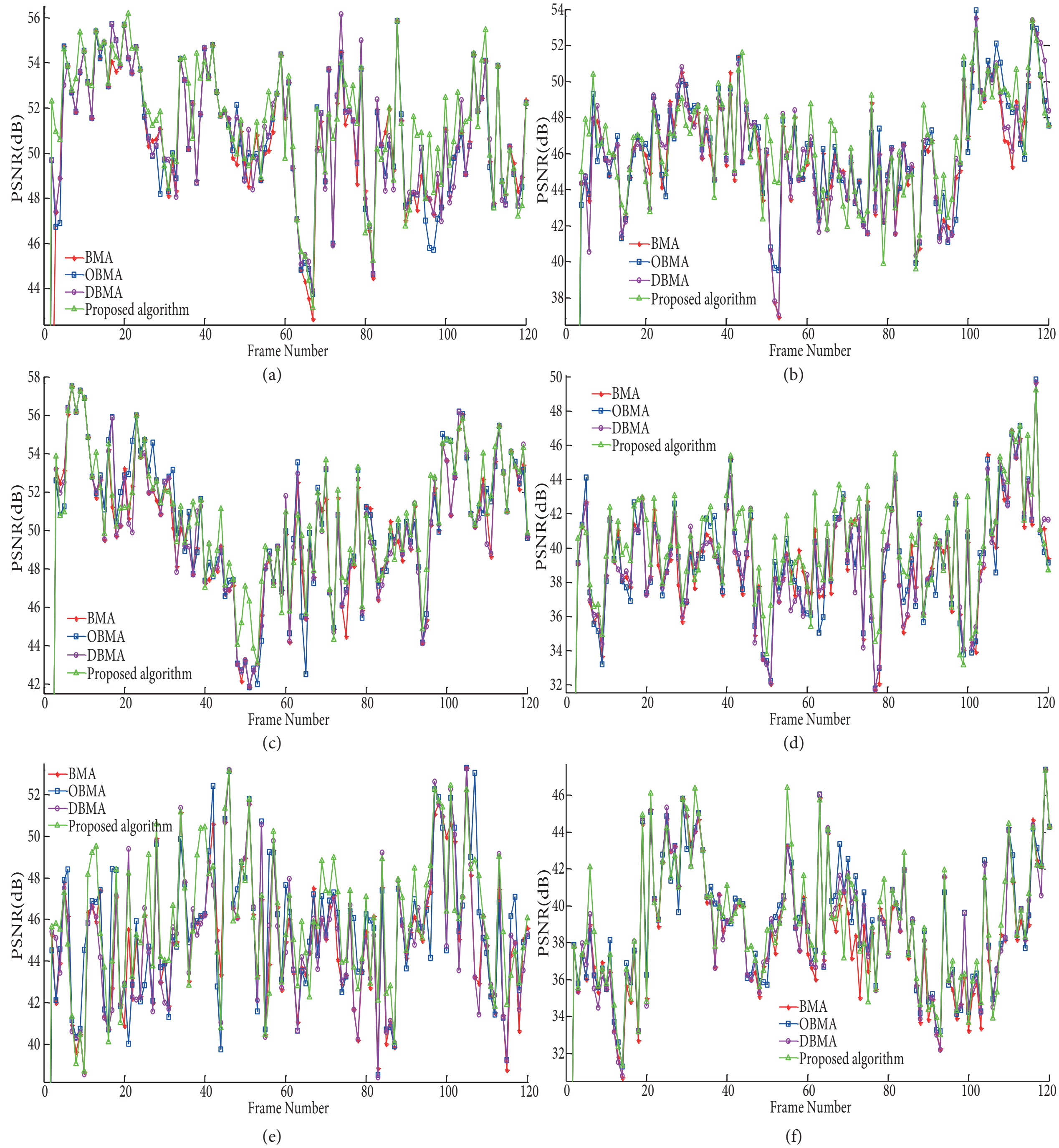

Figure 5. PSNR values of different QCIF video test sequences with average MB missing rate of 20%.

MB causes decreasing error in the boundary matching process. As a result, the estimation of the damaged MV is more accurate. These weights assign less importance to determined directions from the adjacent reconstructed boundaries (results from the last stages of error concealment) and more importance to determined directions from the adjacent error-free boundaries (results from the adjacent error-free MBs). Therefore, even though some of the adjacent MBs of the damaged MB in the current frame have been the error-free MBs, the effect of correct directions improves the boundary matching process.

Figure 6a shows an error-free frame (frame 12) in CIF test sequence “Bus”. Figure 6b shows the damaged frame with average MB missing rate of 20%. The reconstructed frames using the BMA, DBMA, OBMA, and proposed algorithm are shown in Figures 6c–6f, respectively. Figure 7a shows an error-free frame (frame 49) in QCIF test sequence “Suzie”. Figure 7b shows the damaged frame with average MB missing rate of 20%. Figures 7c–7f show the reconstructed frames using the BMA, DBMA, OBMA, and proposed algorithm, respectively. As observed in these figures, the proposed algorithm achieves higher subjective quality over other algorithms.

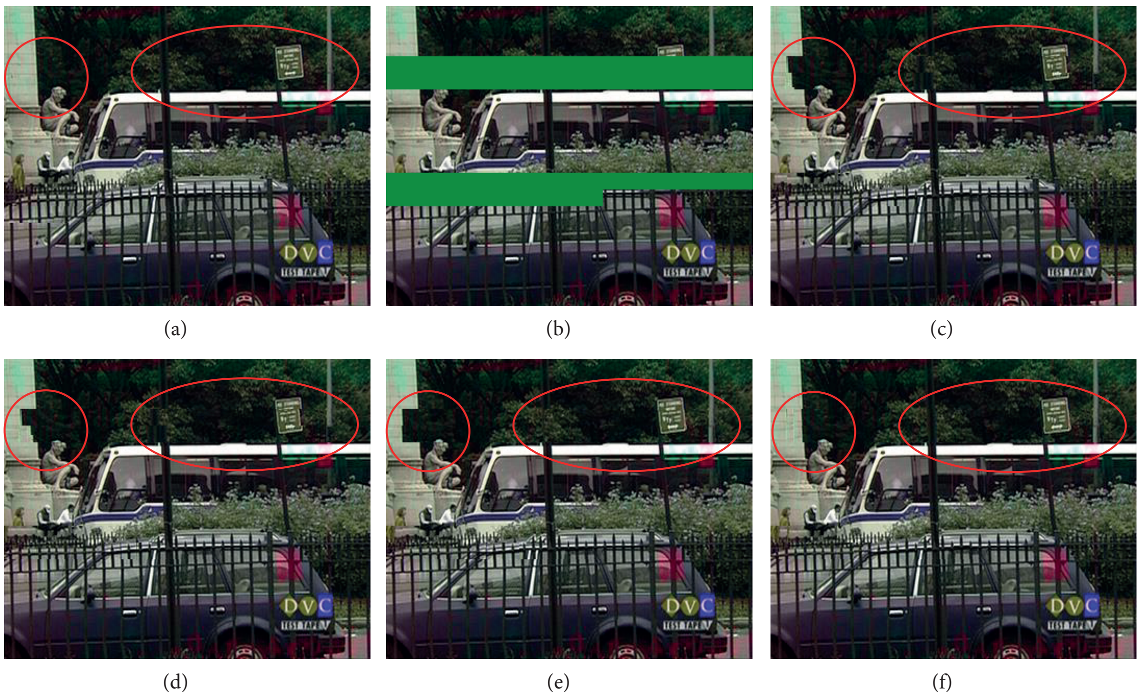

Figure 6. Subjective video quality comparison for frame 13 in CIF video test sequence “Bus” and average MB missing rate of 20%.

5. Conclusion and future work

In this paper, an improved directional boundary matching algorithm was proposed. First, by comparing the outer boundaries of the damaged MB, the proposed algorithm identifies its dominant edge direction. Then it compares boundaries of the candidate MB in the identified direction with adjacent MBs’ boundaries of the damaged MB. Because of direction identification with boundary comparison in outer boundaries of the damaged MB, the algorithm has more accuracy in correct direction identification in the matching process. In addition, this algorithm uses the weighted directional matching function for MVs’ recovery. This weighting causes more accuracy in the estimation of the damaged MV. The experimental results show that the proposed algorithm can improve both objective and subjective quality of reconstructed frames, such as the average PSNR of video test sequences increases, by about 1.37, 1.26, and 1.06 dB in comparison with the BMA, DBMA, and OBMA, respectively.

When the boundary pixels in each adjacent boundary do not have high spatial correlation (i.e. the number of the edges in each damaged MB’s boundary has more than one dominant boundary) or the most adjacent MBs of the damaged MB in the current frame are not valid, the performance of the algorithm may be

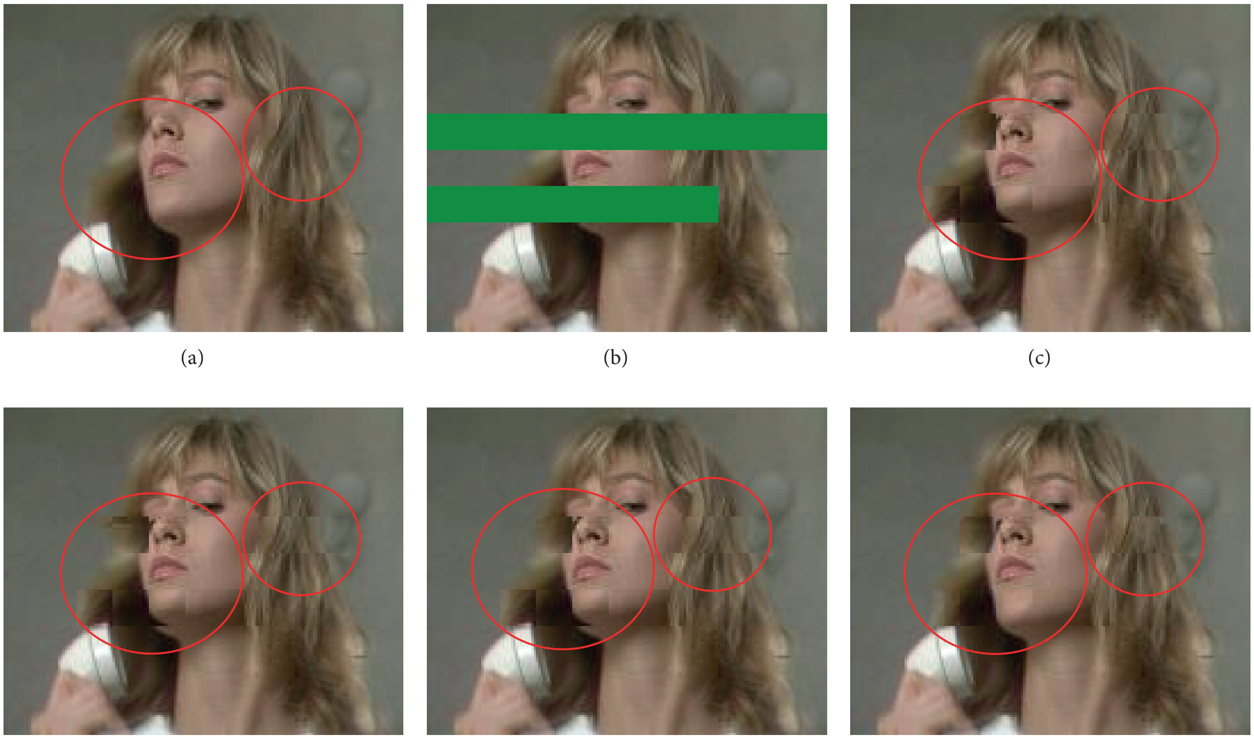

(a) (b) (c) (d) (e) (f)

Figure 7. Subjective video quality comparison for frame 63 in QCIF test sequence "Suzie" and average MB missing rate of 20%.

decreased. In this case, the proposed algorithm can be used with other algorithms, adaptively, which will be included in our future work.

References

[1] Aign S, Fazel K. Temporal and spatial error concealment techniques for hierarchical MPEG-2 video codec. In: IEEE 1995 International Conference on Communications; 18–22 June 1995; Seattle, WA, USA. New York, NY, USA: IEEE. pp. 1778-1783.

[2] Jung Y, Kim Y, Choe Y. Robust error concealment algorithm using iterative weighted boundary matching criterion. In: 2000 International Conference on Image Processing; 10–13 September 2000; Vancouver, BC, Canada. New York, NY, USA: IEEE. pp. 384-387.

[3] Yan B, Ng K. A novel selective motion vector matching algorithm for error concealment in MPEG-4 video transmission over error-prone channels. IEEE T Consum Electr 2003; 49: 1416-1423.

[4] Lee Y, Altunbasak Y, Mersereau R. A temporal error concealment method for MPEG coded video using a multi-frame boundary matching algorithm. In: 2001 International Conference on Image Processing; 7–10 October 2001; Thessaloniki, Greece. New York, NY, USA: IEEE. pp. 990-993.

[5] Min C, Jin S, Oh H, Park S, Jeong J. Temporal error concealment algorithm for H.264/AVC using omnidirectional motion similarity. In: 2010 International Conference on Image Processing Theory Tools and Applications; 7–10 July 2010; Paris, France. New York, NY, USA: IEEE. pp. 144-148.

[6] Park J, Kim J, Lee S. DCT coefficients recovery-based error concealment technique and its application to the MPEG-2 bit stream error. IEEE T Circ Syst Vid 1997; 7: 845-854.

[7] Alkachouh Z, Bellanger M. Fast DCT-based spatial domain interpolation of blocks in images. IEEE T Image Process 2000; 9: 729-732.

[8] Kang LW, Leou JJ. A hybrid error concealment scheme for MPEG-2 video transmission based on best neighborhood matching algorithm. In: IEEE 2004 International Conference on Multimedia and Expo; 27–30 June 2004; Taipei, Taiwan. New York, NY, USA: IEEE. pp. 1355-1358.

[9] Jo M, Kim H, Song W. Hybrid error concealments based on block content. IET Image Process 2007; 1: 141-148.

[10] Ma X, Mu K. Study on the adaptive error concealment technique for mobile video. In: IEEE 2011 International Conference on Communication Software and Networks; 27–29 May 2011; Xi'an, China. New York, NY, USA: IEEE. pp. 276-279.

[11] Haskell P, Messerschmitt D. Resynchronization of motion compensated video affected by ATM cell loss. In: IEEE 1992 International Conference on Acoustics, Speech, and Signal Processing; 23–26 March 1992; San Francisco, CA, USA. New York, NY, USA: IEEE. pp. 545–548.

[12] Chien J, Li G, Chen M. Effective error concealment algorithm of whole frame loss for H.264 video coding standard by recursive motion vector refinement. IEEE T Consum Electr 2010; 56: 1689-1698.

[13] Vazquez M, Garcia-Ramirez A, Ramirez-Acosta A. Image processing for error concealment. In: 2011 Mexican International Conference on Artificial Intelligence; 26 November–4 December 2011; Puebla, Mexico. New York, NY, USA: IEEE. pp. 133-138.

[14] Lam W, Reibman A, Liu R. Recovery of lost or erroneously received motion vectors. In: IEEE 1993 International Conference on Acoustics, Speech, and Signal Processing; 27–30 April 1993; Minneapolis, MN, USA. New York, NY, USA: IEEE. pp. 417-420.

[15] Ai M, Jiang Q. Weighted motion vectors of double candidate blocks based temporal error concealment method for video transmission over wireless network. In: 2010 International Conference on Educational and Network Technology; 25–27 June 2010; Qinhuangdao, China. New York, NY, USA: IEEE. pp. 478-481.

[16] Araghi A, Agahian Panahi M, Kasaei S. Error concealment using wide motion vector space for H.264-AVC. In: 2011 Iranian Conference on Electrical Engineering; 17–19 May 2011; Tehran, Iran. New York, NY, USA: IEEE. pp. 1-6.

[17] Gao Z, Lie W. Video Error Concealment by Using Kalman-Filtering Technique. In: 2004 International Symposium on Circuits and Systems; 23–26 May 2004; Vancouver, BC, Canada. New York, NY, USA: IEEE. pp. 69-72.

[18] Marvasti-Zadeh SM, Ghanei-Yakhdan H, Kasaei S. A novel boundary matching algorithm for video temporal error concealment. International Journal of Image, Graphics, and Signal Processing 2014; 6: 1-10.

[19] Thaipanich T, Wu P, Jay Kuo C. Video error concealment with outer and inner boundary matching algorithms. International Society for Optical Engineering Journal 2007; 6696: 6696-07.

[20] Marvasti-Zadeh SM, Ghanei-Yakhdan H, Kasaei S. Dynamic temporal error concealment for video data in error-prone environments. In: 2013 Iranian Conference on Machine Vision and Image Processing; 10–12 September 2013; Zanjan, Iran. New York, NY, USA: IEEE. pp. 43-47.

[21] Nemethova O, Al-Moghrabi A, Rupp M. An adaptive error concealment mechanism for H.264/AVC encoded low-resolution video streaming. In: 2006 European Signal Processing Conference; 4–6 September 2006; Florence, Italy.

[22] Marvasti-Zadeh SM, Ghanei-Yakhdan H, Kasaei S. An efficient adaptive boundary matching algorithm for video error concealment. Iranian Journal of Electrical & Electronic Engineering 2014; 10: 188-202.

[23] Xiang Y, Feng L, Xie S, Zhou Z. An efficient spatio-temporal boundary matching algorithm for video error concealment. Multimed Tools Appl 2011; 52: 91-103.

[24] Chen X, Chung Y, Bae C. Dynamic multi-mode switching error concealment algorithm for H.264/AVC video applications. IEEE T Consum Electr 2008; 54: 683-695.

[25] Wang Y, Zhu Q. Error control and concealment for video communication: a review. P IEEE 1998; 86: 974-997.

[26] Barjatya A. Block matching algorithms for motion estimation. Final Project Paper, DIP 6620, Spring 2004. Logan, UT, USA: Utah State University, 2004.